

Two-way packing model for ribonuclease T1 fluorescence

Christopher Haydock, Salah S. Sedarous, Franklyn G. Prendergast

Mayo Foundation, Department of Biochemistry and Molecular Biology
200 First St. SW, Rochester, MN 55905

Teresa A. Felmlee

Mayo Foundation, Division of Clinical Microbiology
200 First St. SW, Rochester, MN 55905

ABSTRACT

The fluorescence intensity decay of ribonuclease T1 is biexponential at neutral pH. The lifetimes in nanoseconds and preexponential factors of the exponential components are 3.9 (81%) and 1.7 (19%). The mutations A22L, G23A, L26A, V67G, and V67D, which all neighbor tryptophan-59, have a fairly small effect on this biexponential decay. The lifetime of the long lived component varies from 3.7 to 4.2 nanoseconds and the preexponential varies from 75% to 92%. The emission maximum varies from 319 to 328 nanometers and the acrylamide quenching rate constant varies from 2.0 to $4.0 \times 10^8 \text{ M}^{-1}\text{s}^{-1}$ for these mutations. Minimum perturbation mapping simulations of the tryptophan-59 side chain in wild type ribonuclease T1 show that the χ^2 side chain dihedral angle may adopt either a perpendicular or an antiperpendicular conformation. These computational and spectroscopic results lead us to propose a two-way packing model for tryptophan-59. This model predicts the relative free energies of the perpendicular and antiperpendicular conformations and acrylamide interaction site to indole ring distances for the wild type and mutant ribonucleases.

1 INTRODUCTION

Chen *et al.* have proposed that tryptophan-59 of ribonuclease T1 exists in two conformations within a hydrophobic pocket.¹ Their evidence for this included the biexponential fluorescence intensity decay at neutral pH, the identical fluorescence spectrum and the fivefold differential acrylamide quenching of these lifetime components, and the crystallographic structure of tryptophan-59 and surrounding residues. However, they did not propose two specific conformations for tryptophan-59. A more recent high resolution crystallographic structure of ribonuclease T1 at neutral pH placed tryptophan-59 in a single conformation and gave a reasonable R value and electron density fit.² It is interesting to note that the neighbor residues leucine-26 and valine-78 were found to be disordered. These residues contact opposite ends of the indole ring system within the hydrophobic pocket, see Figure 1. We suspect that this disorder accommodates the two alternative packings of tryptophan-59 within its hydrophobic pocket. Here, we further investigate this two tryptophyl conformation model by computing the indole side chain isomerization energy with the minimum perturbation mapping method.³ Minimum perturbation mapping is based on two approximations. First, it is assumed that the adjustments in protein structure required

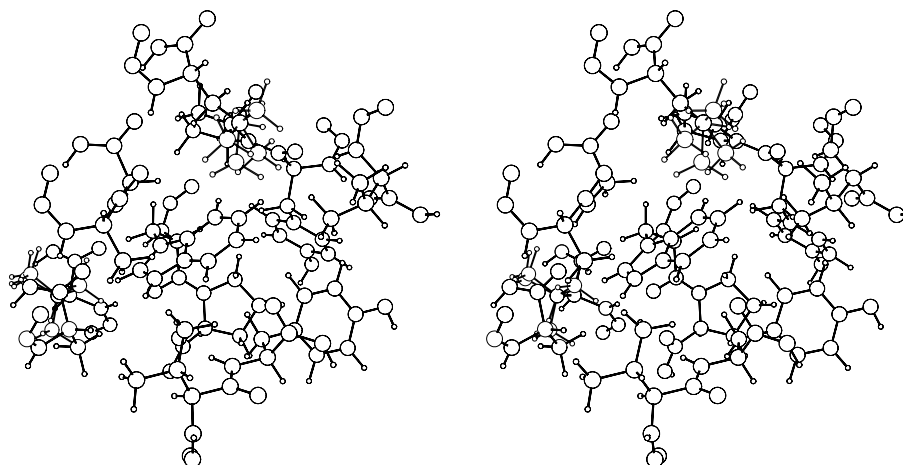


Figure 1: Crystallographic structure of ribonuclease T1 around tryptophan-59. Leucine-26 (top) and valine-78 (lower left) are disordered.

to accommodate multiple side chain conformations are highly localized around the isomerizing side chain. This approximation solves ring bending, secondary transition, and time scale problems usually encountered when computing free energy differences along an isomerization reaction coordinate and provides very smooth estimates of the protein energy and Cartesian coordinates as a function of the isomerization coordinate. The smoothness permits simple expressions for isomerization entropy, transition rate, side chain order parameters, and also leads to a simple method of refining the reaction coordinate. The second approximation is that the side chain isomer energies are pairwise additive. Accordingly, the self energy of a given side chain and the interaction energy of this side chain with each of its neighbors is computed with all other protein side chains truncated at the C^β atom. This approximation results in a greatly simplified calculation of the isomerization probabilities of any given side chain such as tryptophan and apparently permits the simple construction of an ensemble of most probable protein structures.⁴

2 METHODS

Molecular mechanics structures were initially fit to the crystallographic structure with 5 steps of conjugate gradient minimization. These fits removed about 1000 kcal/mol in bond, angle, and van der Waals energy and had a root mean square difference from the crystallographic structure of about 0.05 angstroms. The fits may thus be viewed as a greatly simplified method of fitting a molecular mechanics structure to the crystallographic structure factors. Following truncation of neighbor side chains the protein was partitioned into a free and fixed atoms regions. A variety of truncation and free atoms schemes were investigated. The least computationally expensive scheme truncated leucine-26, valine-33, tyrosine-38, valine-67, tyrosine-68 and valine-78 at the C^β atom. All atoms of these residues and alanine 19 and 22, glycine-23, proline-39, tryptophan-59 and proline-60 as well as interconnecting backbone carbonyl and amide groups were free. More elaborate truncation schemes allowed simultaneous mapping of tryptophan-59 χ^1 *gauche* isomers. These schemes added truncation of some combination of residues glutamine-20, tyrosine-24, lysine-25, tyrosine-57, glutamate-58, serine-69 or valine-79 at the C^β atom and residues alanine-19, valine-78 or phenylalanine-80 at the C^α atom. All minimum perturbation mapping simulations employed the polar hydrogen approximation and the CHARMM version 19 parameters with charges on ionized side chains reduced by 80%.⁵

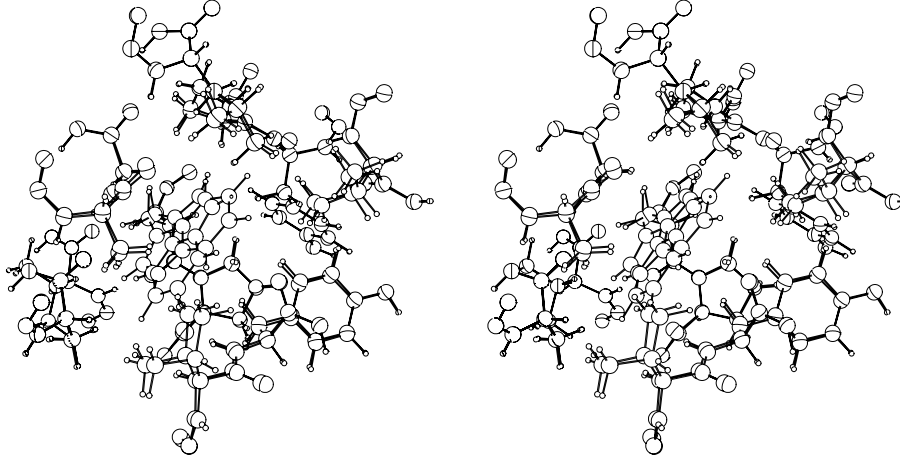


Figure 2: Energy minimized perpendicular (crystallographic) and antiperpendicular conformations of tryptophan-59. All energy minimization free atoms are shown.

Two minimum perturbation energy maps over tryptophan-59 $\chi^1 \times \chi^2$ torsion space were computed for each mutation. One map was computed with the wild type side chain at the mutation position and the other map had the mutated side chain in position. Both maps had all other neighbor residues truncated at the C^β atom. In cases where the wild type or mutant side chain had multiple isomers it was assumed that this side chain would remain in the conformation that had the lowest total energy with the tryptophan-59 perpendicular conformation. This assumption was checked by computing tryptophan maps for every isomer, which showed that the side chain self energy generally made a larger contribution to the total energy than the tryptophan to neighbor interaction energy. Note that the side chain self energy includes the energy of interaction of a side chain with all neighboring backbone and C^β atoms. The minimum perturbation energy maps over tryptophan-59 $\chi^1 \times \chi^2$ torsion space were converted to probability maps and integrated over the perpendicular and antiperpendicular wells. The relative free energy of the antiperpendicular conformation is

$$\Delta A = A_{\text{anti}} - A_{\text{perp}}, \quad (1)$$

where A_{anti} and A_{perp} are the logarithm of the integral over the perpendicular and antiperpendicular probability wells, respectively, times minus the Boltzmann constant times the temperature. The shift in relative free energy due to a mutation is

$$\Delta\Delta A = \Delta A_{\text{mutant}} - \Delta A_{\text{WT}}, \quad (2)$$

where ΔA_{mutant} and ΔA_{WT} are the relative free energies of the antiperpendicular conformations of the mutant and wild type ribonuclease given by Eq. (1). The effect on the aspartate of lowering the pH was simulated by removing the charge on the O^δ atoms.

The fluorescence intensity decay was fit to a multiexponential

$$I(t) = I_0 \sum \alpha_i e^{-t/\tau_i}, \quad \sum \alpha_i = 1, \quad (3)$$

where α_i are the preexponentials and τ_i are the component lifetimes. We assumed that the long lifetime component was associated with the perpendicular conformation and the short lifetime with the antiperpendicular. The experimental relative free energy of the antiperpendicular conformation is

$$\Delta A = -k_B T \ln(\alpha_{\text{anti}}/\alpha_{\text{perp}}), \quad (4)$$

where α_{anti} and α_{perp} are the fluorescence intensity decay preexponential factors of the short and long lifetime components, respectively. The experimental shift in relative free energy of the antiperpendicular conformation is given by Eqs. (2) and (4).

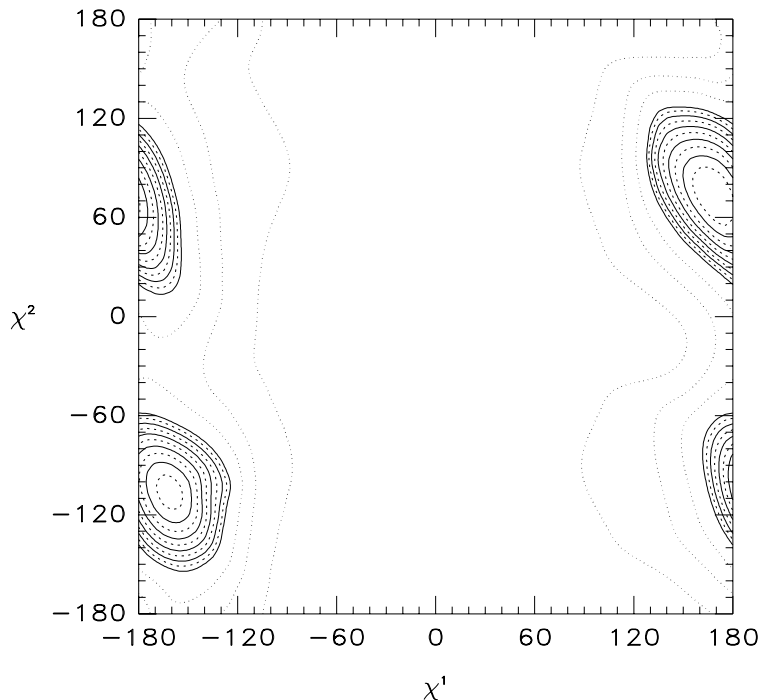


Figure 3: Minimum perturbation mapping of perpendicular (upper well) and antiperpendicular (lower well) conformations of tryptophan-59. Contour levels are *dashed*, 1, 3, 5, 7, 9; *solid*, 2, 4, 6, 8, 10; *dotted*, 15.8, 25.1, 39.8, kcal/mol, where zero corresponds to -451.3 kcal/mol.

In addition to minimum perturbation mapping with truncated neighbor side chains, simple energy minimizations were performed on the perpendicular and antiperpendicular tryptophan-59 conformations with all neighbor side chains intact and in their crystallographic conformations. The Leucine-26 χ^2 and Valine-78 χ^1 dihedral angles were in the *gauche*⁺ and *trans* conformations, respectively. These simple energy minimization calculations treated all hydrogen atoms explicitly and used the CHARMM version 22 revision b3 parameters. The free atoms were the same as those in the least computationally expensive minimum perturbation mapping scheme plus the side chain atoms of the same residues and nonpolar hydrogens. Distances from the pyrrole and benzol rings of indole to the Lee and Richards solvent surface were computed by a small program that examined dot surface files.⁶

3 RESULTS AND DISCUSSION

The results of the simple energy minimization on the perpendicular and antiperpendicular tryptophan-59 conformations are shown in Figure 2. The energies of these structures differ by less than 1 kcal/mol. The indole ring systems of the two conformations overlap surprisingly well, since it might be expected that for perpendicular and antiperpendicular conformations the pyrrole ring would simply flip over with little change in position and the benzol rings would project outwards in opposite directions. The subtlety of the placement of the indole ring is further emphasized by the tiny differences in backbone and neighbor side chain atom positions between

the two conformations. These results build confidence that the existence of perpendicular and antiperpendicular conformations is not an artifact of the approximations of minimum perturbation mapping.

	Theory	Experiment
A22L	0.4	-0.2
G23A	-0.2	0.3
L26A	1.3	0.6
V67G	0.1	-0.1
V67D	5	0.3
V67D (pH 5.0)	2	-0.3

Table 1: Free energy shifts (kcal/mol) of the tryptophan-59 antiperpendicular conformation relative to the perpendicular conformation for ribonuclease T1 mutants. Experimental shifts are based on fluorescence intensity decay preexponentials.

Figure 3 shows the minimum perturbation mapping over tryptophan-59 $\chi^1 \times \chi^2$ torsion space with all neighbor side chains truncated. The tryptophan *gauche* isomers are not included on this map. Maps with a wild type or mutant side chain in position (not shown) are very similar in appearance, except that the perpendicular and antiperpendicular wells differ in depth by a few tenths of a kcal/mol. The theoretical and experimental free energy shifts of the antiperpendicular tryptophan conformation of five ribonuclease T1 mutants are shown in Table 1. Both the theoretical and experimental results show the small effect of these mutations on the fluorescence intensity decay. Free energy shifts of this magnitude require careful measurement and are certainly difficult to calculate theoretically. The large shifts predicted for the aspartate mutant reflect the inadequacies of the distance dependent dielectric and reduced charge electrostatic model. In agreement with experiment, lowering the pH is predicted to stabilize the antiperpendicular tryptophan conformation.

	Interaction site 1				Interaction site 2				k_q ($M^{-1}s^{-1}$)
	Pyrrole		Benzol		Pyrrole		Benzol		
	Perp.	Anti.	Perp.	Anti.	Perp.	Anti.	Perp.	Anti.	
WT	5.2	5.1	3.7	3.8	3.6	5.3	4.9	3.5	2.1×10^8
A22L	5.8	5.2	3.9	4.4	3.6	5.3	4.9	3.5	3.3×10^8
G23A	5.2	5.1	3.7	3.8	3.6	5.3	4.9	3.5	2.5×10^8
L26A	4.5	3.3	3.3	3.3	3.6	5.3	4.9	3.5	2.4×10^8
V67G	4.8	4.7	3.5	3.4	3.7	5.4	5.0	3.6	4.0×10^8
V67D	4.8	4.7	3.5	3.4	3.6	5.3	4.9	3.5	2.1×10^8

Table 2: Distance (\AA) from indole rings to the Lee and Richards protein surface constructed with a 1.4 \AA probe radius and acrylamide quenching rate constants for ribonuclease T1 wild type and mutants.

The acrylamide quenching rate for the long lifetime fluorescence intensity decay component of ribonuclease T1 at neutral pH is $1.55 \times 10^8 M^{-1}s^{-1}$ and for the short component is $8.89 \times 10^8 M^{-1}s^{-1}$.¹ If the quenching process is electron transfer, the distance from the acrylamide interaction site to the indole ring should be about an angstrom shorter when tryptophan is in the antiperpendicular conformation. There are two potential quencher interaction sites. Interaction site 1 approaches tryptophan-59 from the direction of the viewer in Figure 1 or 2 and site 2 approaches from below. In the crystallographic structure water molecule number 107 is positioned in site 2 with a low temperature factor.² Table 2 shows the distance from each acrylamide interaction site to the indole rings of tryptophan-59 in the perpendicular and antiperpendicular conformation. The distances are given for both the pyrrole and benzol rings of indole. It is apparent from the results in Table 2 that an orientation effect is required to explain the difference in electron transfer efficiency to the perpendicular and antiperpendicular conformations.

The distance from the center of a 1.4 angstrom probe at site 1 to the nearest indole atom is 3.7 or 3.8 angstroms in either the perpendicular and antiperpendicular conformation and from site 2 is 3.5 or 3.6 angstroms. The shortest distance from site 1 is always to the benzol ring. However, site 2 is closer to the pyrrole ring in the perpendicular conformation and the benzol ring in the antiperpendicular conformation. Thus the higher quenching rate of the short lifetime component could be explained by an orientation effect that favors electron transfer to the benzol ring from site 2. Both the surface to ring distances and average quenching rates shown in Table 2 for the mutant ribonucleases suggest that the acrylamide quenching mechanism will be very similar to the wild type.

4 CONCLUSIONS

The results presented here suggest that the two-way packing model is a promising model for explaining the fluorescence intensity decay of ribonuclease T1. A further test of this model would be to measure the kinetics of tryptophan-59 interconversion between the perpendicular and antiperpendicular conformation. This rate is likely to be somewhere in the range of milliseconds to tens of seconds. Since the fluorescence intensity decay preexponential factors are pH dependent, the interconversion rate could probably be measured in a stopped-flow pH jump experiment. Another important test would be to solve the crystallographic structure and include the explicit possibility of two-way packing of tryptophan-59.

5 ACKNOWLEDGMENTS

This work is supported in part by the W. M. Keck Foundation and GM 34847.

6 REFERENCES

- [1] L. X.-Q. Chen, J. W. Longworth, and G. R. Fleming. "Picosecond time-resolved fluorescence of ribonuclease T1: A pH and substrate analogue binding study," *Biophys. J.*, 51:865-873, 1987.
- [2] J. Martinez-Oyanedel, H.-W. Choe, U. Heinemann, and W. Saenger. "Ribonuclease T₁ with free recognition and catalytic site: Crystal structure analysis at 1.5 Å resolution," *J. Mol. Biol.*, 222:335-352, 1991.
- [3] C. Haydock. "Protein side chain rotational isomerization: A minimum perturbation mapping study," *J. Chem. Phys.*, 98:8199-8214, 1993.
- [4] J. Desmet, M. De Maeyer, B. Hazes, and I. Lasters. "The dead-end elimination theorem and its use in protein side-chain positioning," *Nature*, 356:539-542, 1992.
- [5] B. R. Brooks, R. E. Bruccoleri, B. D. Olafson, D. J. States, S. Swaminathan, and M. Karplus. "CHARMM: A program for macromolecular energy, minimization, and dynamics calculations," *J. Comput. Chem.*, 4:187-217, 1983.
- [6] B. Lee and F. M. Richards. "The interpretation of protein structures: Estimation of static accessibility," *J. Mol. Biol.*, 55:379-400, 1971.